Numerical Solution of Unsteady Viscous Compressible Fluid Flow along a Porous Plate with Induced Magnetic Field

*Muhammad Minarul Islam, *Md. Tusher Mollah, *Mohammad Sanjeed Hasan, **Md. Mahmud Alam

* Department of Mathematics, Bangabandhu Sheikh Mujibur Rahman Science and Technology University, Gopalganj-8100, Bangladesh,

(minarul_math@yahoo.com, tusher.bsmrstu@gmail.com, sanjeedlhasan@gmail.com)

** Mathematics Discipline, Khulna University,

Khulna-9208, Bangladesh, (alam_mahmud2000@yahoo.com)

Abstract

The unsteady viscous compressible boundary layer fluid flow past a semi-infinite vertical porous plate surrounded in a porous medium with induced magnetic field has been studied numerically. The governing non-linear coupled partial differential equations have been transformed by using usual transformations. The obtained non-linear dimensionless coupled partial differential equations have been solved numerically. The explicit finite difference method is used as solution technique and MATLAB software is used as a secondary tool. The obtained results for the density, velocity, induced magnetic field as well as temperature distributions are shown graphically.

Key words

MHD, Porous medium, Induced magnetic field, Finite difference method, Heat transfer.

1. Introduction

The field of magneto-hydrodynamics has been concerned with geophysical and astrophysical problems for several numbers of years. The combined heat transfer consideration arises due to buoyancy forces instigated by thermal diffusions. Condensing and boiling are characteristic for many separation processes in chemical engineering as drying, evaporation, distillation,

condensation, rectification and absorption of a fluid. In recent times, the MHD is used to affect a flow stream of an electrically conducting fluid for the resolution of thermal protection, braking, propulsion and control. The general boundary layer equations for continuous surfaces have been analyzed by Sakiadis (1961). Due to the importance of the flow past a continuously moving surface in manufacturing processes such as hot rolling, metal and plastic extrusion, continuous casting, glass fiber and paper production, the steady heat transfer flow past a continuously moving plate with variable temperature has been analyzed by Soundalgekar and Ramana Murty (1980). Along with the possessions of magnetic field, the effect of transpiration parameter, being an effective method of controlling the boundary layer has been considered by Kafoussias (1991). The combined boundary layer heat and mass transfer of an electrically conducting fluid in MHD natural convection adjacent to a vertical surface has been analyzed by Chen (2004). Alam et al. (2006) numerically examined the mass transfer flow past a vertical porous medium with heat generation and thermal diffusion on the combined free-forced convection under the influence of transversely applied magnetic field. The level of concentration of foreign mass has been assumed very low in this study so that the thermal and mass diffusion were neglected. They used perturbation technique to obtain the solution. Such type of model studies have been carried out by many investigators such as Sattar and Alam (1999) and Alam et al. (2006). The effects of hall current and viscous dissipation on MHD free convection fluid flow in a rotating system have been studied by Quader and Alam (2015). Pervin and Alam (2015) studied the fluid flow through parallel plates in the presence of hall current with inclined magnetic field in a rotating system. The unsteady heat transform of viscous incompressible boundary layer fluid flow through a porous plate with induced magnetic field, and the related problems have been observed by Islam et al. (2016). MHD free convection and mass transfer flow through a vertical oscillatory porous plate in a rotating porous medium with hall, ion-slip currents and heat source have been investigated by Hossain, Samad and Alam (2016).

Hence our aim is to study unsteady viscous compressible fluid flow along a porous plate with induced magnetic field. The explicit finite difference technique has been used to solve the dimensionless equations. The obtained results have been shown in graph.

2. The Basic Governing Equations

The equation of continuity for a viscous compressible fluid in vector form is given as follows:

$$\frac{\partial \rho}{\partial t} + \nabla \rho . \mathbf{q} + \rho \nabla . \mathbf{q} = 0 \tag{1}$$

where ρ is the density of the fluid and $\mathbf{q}$ is the velocity of fluid.

The Navier-Stokes' momentum equation for a viscous compressible fluid when the fluid moves along a porous medium also electrically conducting fluid moves through a magnetic field of intensity $\mathbf{H}$ in vector form is given as follows:

$$\frac{\partial \mathbf{q}}{\partial t} + (\mathbf{q}.\nabla)\mathbf{q} = \mathbf{F} - \frac{1}{\rho}\nabla p + \frac{\upsilon}{3}\nabla(\nabla.\mathbf{q}) + \upsilon \nabla^2 \mathbf{q} - \frac{\upsilon}{k'}\mathbf{q} + \frac{\mu_e}{\rho}(\nabla \wedge \mathbf{H}) \wedge \mathbf{H} \tag{2}$$

where υ is the kinematic viscosity, k' is the permeability of the porous medium, $\mathbf{B}$ is the magnetic field and μ_e is called the magnetic permeability.

The MHD energy equation for a viscous compressible electrically conducting fluid with diffusion thermo is given as follows:

$$\frac{\partial T}{\partial t} + (\mathbf{q}.\nabla)T = \frac{\kappa}{c_p \rho}(\nabla^2 T) + \frac{1}{\sigma c_p \rho}(\nabla \wedge \mathbf{H}).(\nabla \wedge \mathbf{H}) + \Phi \tag{3}$$

where

$$\Phi = \frac{\upsilon}{c_p}\left[2\left\{ \left(\frac{\partial u}{\partial x}\right)^2 + \left(\frac{\partial v}{\partial y}\right)^2 + \left(\frac{\partial w}{\partial z}\right)^2 \right\} - \frac{2}{3}\left(\frac{\partial u}{\partial x} + \frac{\partial v}{\partial y} + \frac{\partial w}{\partial z}\right)^2 + \left(\frac{\partial u}{\partial y} + \frac{\partial v}{\partial x}\right)^2 + \left(\frac{\partial v}{\partial z} + \frac{\partial w}{\partial y}\right)^2 + \left(\frac{\partial w}{\partial x} + \frac{\partial u}{\partial z}\right)^2 \right]$$

The MHD induction equation is given as follows:

$$\frac{\partial \mathbf{H}}{\partial t} = \nabla \wedge (\mathbf{q} \wedge \mathbf{H}) + \frac{1}{\sigma \mu_e}\nabla^2 \mathbf{H} \tag{4}$$

where σ is the electrical conductivity.

3. Mathematical Formulation

Initially the plate as well as the fluid are at the same temperature $T(=T_\infty)$ everywhere. Also it is assumed that the fluid and the plate is at rest initially in its own plane and instantaneously at time $t > 0$, the temperature of the plate is raised to $T_w (> T_\infty)$, which is there after maintained constant, where T_w is the temperature at the wall and T_∞ is the temperature of the species out side the boundary layer. The physical configuration of the study is given in figure 1.
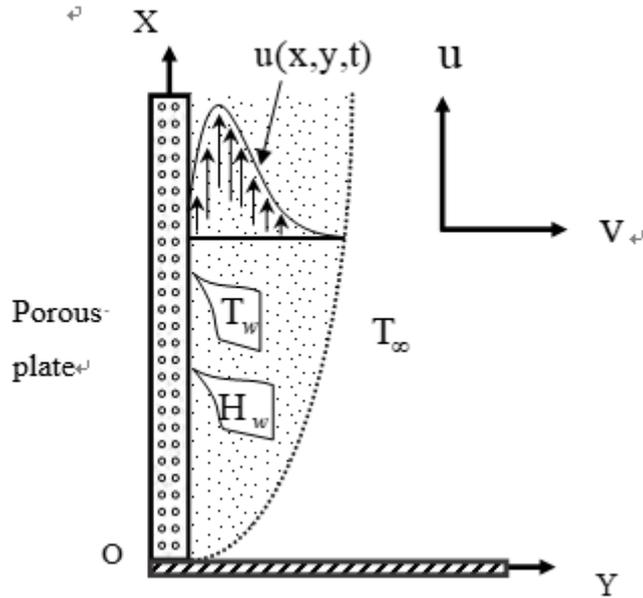
Fig. 1. Physical Configuration and Coordinate System

Within the basis of the above assumptions, the equations related to the unsteady two-dimensional problem governed by the following system of coupled non-linear partial differential equations under the boundary-layer approximations, equations (1) (2) (3) and (4) become

Continuity equation:

$$\frac{\partial \rho}{\partial t} + \rho \frac{\partial u}{\partial x} + \rho \frac{\partial v}{\partial y} + u \frac{\partial \rho}{\partial x} + v \frac{\partial \rho}{\partial y} = 0 \tag{5}$$

Momentum equation:

$$\frac{\partial u}{\partial t} + u \frac{\partial u}{\partial x} + v \frac{\partial u}{\partial y} = g\beta(T - T_\infty) + \frac{1}{3}\upsilon\left(\frac{\partial^2 u}{\partial x^2} + \frac{\partial^2 v}{\partial x \partial y}\right) - \frac{\upsilon}{k'}u + \upsilon \frac{\partial^2 u}{\partial y^2} + \frac{\mu_e}{\rho}H_0 \frac{\partial H_x}{\partial y} \tag{6}$$

$$\frac{1}{3}\upsilon\left(\frac{\partial^2 u}{\partial x \partial y} + \frac{\partial^2 v}{\partial y^2}\right) - \frac{\mu_e}{\rho}H_x \frac{\partial H_x}{\partial y} + \upsilon \frac{\partial^2 v}{\partial y^2} = 0 \tag{7}$$

Magnetic induction equation:

$$\frac{\partial H_x}{\partial t} + v \frac{\partial H_x}{\partial y} = H_0 \frac{\partial u}{\partial y} - H_x \frac{\partial v}{\partial y} + \frac{1}{\sigma\mu_e}\frac{\partial^2 H_x}{\partial y^2} \tag{8}$$

Energy equation:

$$\frac{\partial T}{\partial t} + u \frac{\partial T}{\partial x} + v \frac{\partial T}{\partial y} = \frac{\kappa}{c_p \rho}\frac{\partial^2 T}{\partial y^2} + \frac{1}{\rho c_p \sigma}\left(\frac{\partial H_x}{\partial y}\right)^2 + \frac{\upsilon}{c_p}\left(\frac{\partial u}{\partial y}\right)^2 \tag{9}$$

and the corresponding initial and boundary conditions for the problem are as follows:

$$t = 0, \ u = 0, v = 0, H_x = 0, T \to T \text{ everywhere} \tag{10}$$

$$t > 0, \ u = 0, v = 0, H_x = 0, T \to T_\infty \text{ at } x = 0$$

$$u = 0, v = 0, H_x = H_w, T = T_w \text{ at } y = 0 \tag{11}$$

$$u = 0, v = 0, H_x = 0, T \to T_\infty \text{ at } y \to \infty$$

where x, y are Cartesian coordinate system; u, v are x, y component of flow velocity respectively g is the local acceleration due to gravity; β is the thermal expansion coefficient; υ is the kinematic viscosity; μ_e is the magnetic permeability; ρ is the density of the fluid; H_0 is the constant induced magnetic field; H_x is the X component induced magnetic field and H_w is the induced magnetic field at the wall.

Since the solution of the governing equation (5) to (9) under the initial condition (10) and boundary condition (11) will be based on the finite difference method it is required to make the equations into dimensionless equations.

The dimensionless quantities are as follows:

$$\rho^* = \frac{\mu}{\upsilon}\rho, \tau = \frac{U_0^2}{\upsilon}t, U = \frac{u}{U_0}, V = \frac{v}{U_0}, X = \frac{U_0}{\upsilon}x, Y = \frac{U_0}{\upsilon}y, \theta = \frac{T - T_\infty}{T_W - T_\infty}, \bar{H}_x = \sqrt{\frac{\mu_e \upsilon}{\mu}}\frac{H_x}{U_0}$$

$$G_r = \frac{\upsilon g \beta (T - T_\infty)}{U_0^3} \text{ (Grashof number)}, \quad P_m = \upsilon \sigma \mu_e \text{ (Magnetic diffusivity number)}$$

$$P_r = \frac{\mu c_p}{k} \text{ (Prandtl number)}, E_C = \frac{U_0^2}{c_p(T_W - T_\infty)} \text{ (Eckert number)}$$

$$M = \frac{H_0}{U_0}\sqrt{\frac{\mu_e \upsilon}{\mu}} \text{ (Magnetic force number)}$$

$$k_0 = \frac{\upsilon^2}{kU_0^2} \text{ (Dimensionless permeability of porous medium)}$$

The obtained dimensionless differential equations are as follows:

$$\frac{\partial \rho^*}{\partial \tau} + \rho^* \frac{\partial U}{\partial X} + \rho^* \frac{\partial V}{\partial Y} + U \frac{\partial \rho^*}{\partial X} + V \frac{\partial \rho^*}{\partial Y} = 0 \tag{12}$$

$$\frac{\partial U}{\partial \tau} + U \frac{\partial U}{\partial X} + V \frac{\partial U}{\partial Y} = G_r \theta - k_0 U + \frac{1}{3}\left(\frac{\partial^2 U}{\partial X^2} + \frac{\partial^2 V}{\partial X \partial Y}\right) + \frac{\partial^2 U}{\partial Y^2} + M \frac{\partial \bar{H}_x}{\partial Y} \tag{13}$$

$$\frac{4}{3}\frac{\partial^2 V}{\partial Y^2} = \bar{H}_x \frac{\partial \bar{H}_x}{\partial Y} - \frac{1}{3}\frac{\partial^2 U}{\partial X \partial Y} \tag{14}$$

$$\frac{\partial \bar{H}_x}{\partial \tau} + V \frac{\partial \bar{H}_x}{\partial Y} = M \frac{\partial U}{\partial Y} - \bar{H}_x \frac{\partial V}{\partial Y} + \frac{1}{P_m}\frac{\partial^2 \bar{H}_x}{\partial Y^2} \tag{15}$$

$$\frac{\partial \theta}{\partial \tau} + U \frac{\partial \theta}{\partial X} + V \frac{\partial \theta}{\partial Y} = \frac{1}{P_r}\frac{\partial^2 \theta}{\partial Y^2} + E_c\left(\frac{\partial U}{\partial Y}\right)^2 + \frac{E_c}{P_m}\left(\frac{\partial \bar{H}_x}{\partial Y}\right)^2 \tag{16}$$

Also the associated initial (10) and boundary (11) conditions become

$$\tau = 0, \quad U = 0, V = 0, \bar{H}_x = 0, \theta = 0 \text{ everywhere} \tag{17}$$

$$\tau > 0, \quad U = 0, V = 0, \bar{H}_x = 0, \theta = 0 \text{ at } X = 0$$

$$U = 0, V = 0, \bar{H}_x = 1, \theta = 1 \text{ at } Y = 0 \tag{18}$$

$$U = 0, V = 0, \bar{H}_x = 0, \theta = 0 \text{ at } Y \to \infty$$

4. Numerical Solution

To solve the dimensionless system (12) to (16) by the explicit finite difference method subject to the boundary conditions, a set of finite difference equations is required. For which, the region within the boundary layer is divided into a grid or mesh of lines parallel to X and Y axes where X-axis is taken along the plate and Y-axis is normal to the plate as shown in figure-1.

Here we consider that the plate of height $X_{max} (=100)$ i.e. X varies from 0 to 100 and regard $Y_{max} (=30)$ as corresponding to $Y \to \infty$ i.e. Y varies from 0 to 30. We take $m = 200$ and $n = 60$ grid spacing in the X and Y directions respectively.

It is assumed that ΔX, ΔY are constant mesh sizes along X and Y directions respectively and taken as follows:

$$\Delta X = 0.5 (0 \le x \le 100)$$

$$\Delta Y = 0.5 (0 \le y \le 30)$$

with the smaller time-step, $\Delta \tau = 0.005$

Let $\rho^{*\prime}$, U', θ' and $\bar{H}'$ denote the values of ρ^*, U, θ and $\bar{H}$ at the end of a time-step respectively. Using the explicit finite difference approximation the following appropriate set of finite difference equations are obtained as:

$$\frac{\rho^{*\prime}_{i,j} - \rho^*_{i,j}}{\Delta \tau} + \rho^*_{i,j} \frac{U_{i,j} - U_{i-1,j}}{\Delta X} + \rho^*_{i,j} \frac{V_{i,j} - V_{i,j-1}}{\Delta Y} + U_{i,j} \frac{\rho^*_{i,j} - \rho^*_{i-1,j}}{\Delta X} + V_{i,j} \frac{\rho^*_{i,j} - \rho^*_{i,j-1}}{\Delta Y} = 0 \tag{19}$$

$$\frac{U'_{i,j} - U_{i,j}}{\Delta \tau} + U_{i,j} \frac{U_{i,j} - U_{i-1,j}}{\Delta X} + V_{i,j} \frac{U_{i,j} - U_{i,j-1}}{\Delta Y} = G_r \theta_{i,j} - k_0 U_{i,j}$$
$$+ \frac{1}{3} \left(\frac{U_{i+1,j} - 2U_{i,j} + U_{i-1,j}}{(\Delta X)^2} + \frac{V_{i+1,j+1} - V_{i+1,j-1} - V_{i-1,j+1} + V_{i-1,j-1}}{4\Delta X \Delta Y} \right) \tag{20}$$
$$+ \frac{U_{i,j+1} - 2U_{i,j} + U_{i,j-1}}{(\Delta Y)^2} + M \frac{\bar{H}_{i,j} - \bar{H}_{i,j-1}}{\Delta Y}$$

$$\frac{4}{3} \frac{V_{i,j+1} - 2V_{i,j} + V_{i,j-1}}{(\Delta Y)^2} = \bar{H}_{i,j} \frac{\bar{H}_{i,j} - \bar{H}_{i,j-1}}{\Delta Y} - \frac{1}{3} \frac{U_{i+1,j+1} - U_{i+1,j-1} - U_{i-1,j+1} + U_{i-1,j-1}}{4\Delta X \Delta Y} \tag{21}$$

$$\frac{\bar{H}'_{i,j} - \bar{H}_{i,j}}{\Delta\tau} + V_{i,j}\frac{\bar{H}_{i,j} - \bar{H}_{i,j-1}}{\Delta Y} = M\frac{U_{i,j} - U_{i,j-1}}{\Delta Y} - \bar{H}_{i,j}\frac{V_{i,j} - V_{i,j-1}}{\Delta Y} + \frac{1}{P_m}\frac{\bar{H}_{i,j+1} - 2\bar{H}_{i,j} + \bar{H}_{i,j-1}}{(\Delta Y)^2} \quad (22)$$

$$\frac{\theta'_{i,j} - \theta_{i,j}}{\Delta\tau} + U_{i,j}\frac{\theta_{i,j} - \theta_{i-1,j}}{\Delta X} + V_{i,j}\frac{\theta_{i,j} - \theta_{i,j-1}}{\Delta Y} = \frac{1}{P_r}\frac{\theta_{i,j+1} - 2\theta_{i,j} + \theta_{i,j-1}}{(\Delta Y)^2}$$
$$+ E_c\left(\frac{U_{i,j} - U_{i,j-1}}{\Delta Y}\right)^2 + \frac{E_c}{P_m}\left(\frac{\bar{H}_{i,j} - \bar{H}_{i,j-1}}{\Delta Y}\right)^2 \quad (23)$$

and the initial and boundary conditions with the finite difference scheme are given as follows:

$$U_{i,j}^0 = 0, \quad V_{i,j}^0 = 0, \quad \theta_{i,j}^0 = 0, \quad \bar{H}_{i,j}^0 = 0, \quad (24)$$

$$U_{0,j}^n = 0, \quad V_{0,j}^n = 0, \quad \theta_{0,j}^0 = 0, \quad \bar{H}_{0,j}^n = 0,$$

$$U_{1,0}^n = 0, \quad V_{i,0}^n = 0, \quad \theta_{i,0}^n = 1, \quad \bar{H}_{i,0}^n = 1, \quad (25)$$

$$U_{i,L}^n = 0, \quad V_{i,L}^n = 0, \quad \theta_{i,L}^n = 0, \quad \bar{H}_{i,L}^n = 0, \quad \text{where } L \to \infty$$

Here the subscripts i and j designate the grid points with x and y coordinates respectively and the superscript n represents a value of time, $\tau = n\Delta\tau$ where $n = 0, 1, 2,....$

5. Results and Discussion

5.1 Justification of Grid Space

To verify the effects of grid space for m and n, the computations have been carried out for three different grid spaces such as $m=100, n=30$; $m=150, n=50$ and $m=200, n=60$ are shown in figure-2. It is seen that the graph for $m=200, n=60$ is more shaded than others. According to this situation, the results of density, velocity, temperature and magnetic induction have been carried out for $m=200$ and $n=60$.

5.2 Steady State Solution

In order to verify the effects of time step size $\Delta\tau$, the computations have been carried out for five different time step sizes such as $\tau = 10, 20, 70, 80, 90$. It is observed that, the result of computations for ρ, U, θ and H_x, however shows so little changes after $\tau = 70$. Thus the solutions of all variables for $\tau = 80$ are essentially the steady-state solutions which is shown in figure-3. Hence the density, velocity, temperature and magnetic induction profiles have been carried out for $\tau = 80$.
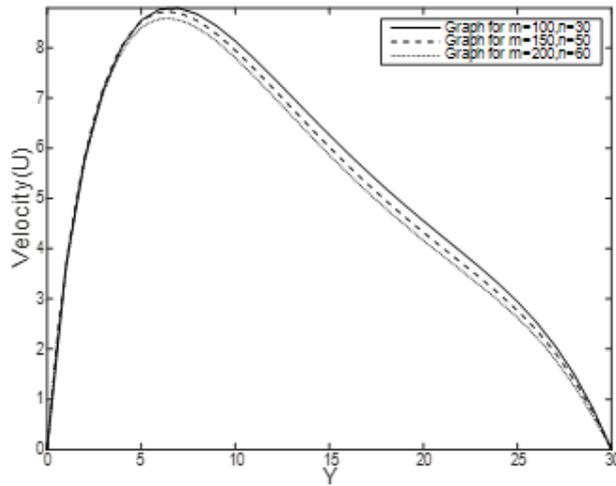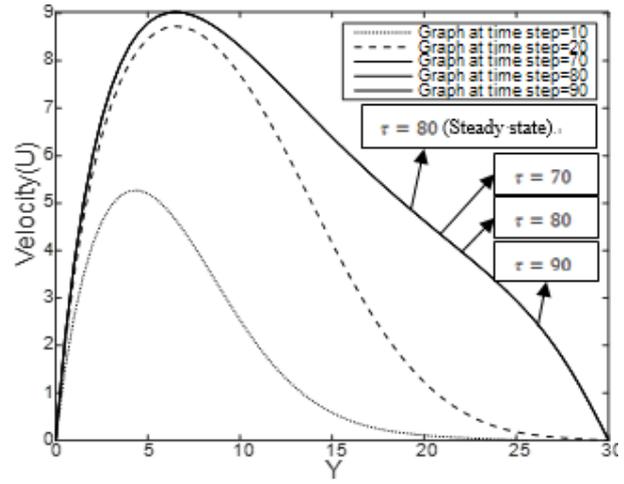
Fig. 2. Velocity for Different Grid Spaces

Fig. 3. Velocity for Different Time Steps

Due to analyze the physical situation of the model, we have computed the steady state numerical values of the non-dimensional density ρ, velocity U, temperature θ and magnetic induction H within the boundary layer for different values of Grashof number (G_r), Prandtl number (P_r), Eckert number (E_c), Magnetic diffusivity number (P_m), Magnetic force number (M) and permeability of Porous plate (k_0).

Here the solution for $\tau = 80$ are essentially steady state solutions. For the purpose of special importance of cooling problem in nuclear engineering in connection with the cooling of reactors, the value of the Grashof number for heat transfer is taken to be positive $(G_r > 0)$ and the present study has considered $G_r = 2.0,\ 2.5,\ 3.0$ also take the value of density of air at 0° C is 1.293 kg m^3. Since the study is related to compressible fluid, we have chosen atmospheric air whose $P_r = 0.71$ (Prandtl number for air at 20°C), and have also taken lower Prandtl number as air such as $P_r = 0.5,\ 0.6$. Here the investigation are assumed for both lighter and heavier fluid particles, hence with respect to the convergence criteria of the problem the values of parameters M, P_m and E_c are chosen arbitrarily as $M = 0.01$, $P_m = 1.0$, $E_c = 0.001,\ 0.005$ and 0.008 also the dimensionless permeability of porous medium $\kappa_0 = 0.21$ are considered as a fixed value. Along with the obtained steady state solutions, the flow behaviors in case of cooling problem are discussed graphically. The profiles of the density, velocity, temperature and magnetic field versus Y are illustrated in (Figures 4-6).
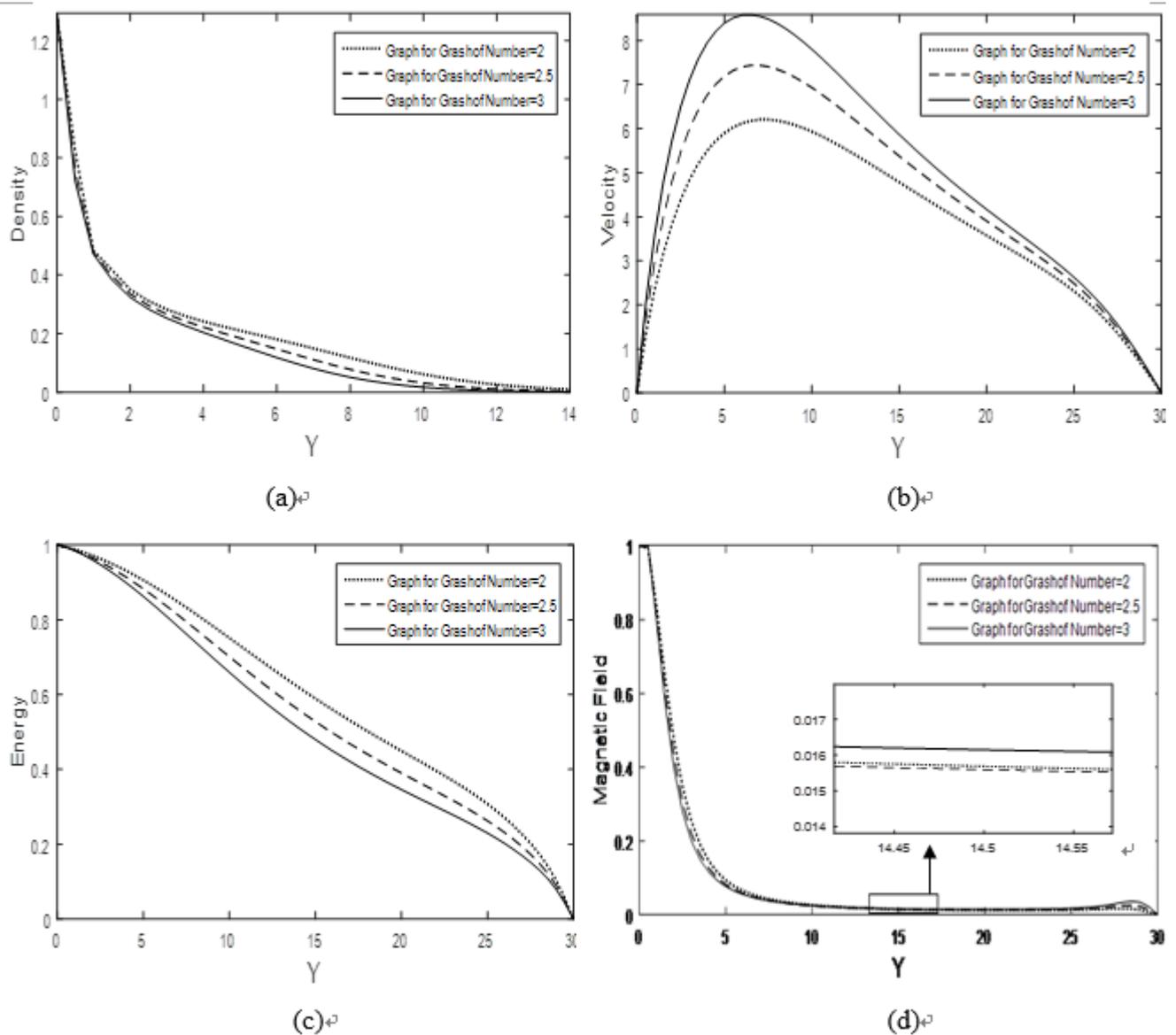
Fig. 4. Effect of Grashof number on: (a) Density; (b) Velocity; (c) Energy; (d) Magnetic Induction, where $M = 0.01, P_m = 1.00, k_0 = 0.21, P_r = 0.71, E_c = 0.001$, at time $\tau = 80$ (Steady state).

Figure-4 shows the profiles of density (ρ), energy (θ), and magnetic induction (H) decreases with increase of Grashof number (G_r), also the velocity profiles increases with increase of Grashof number (G_r).
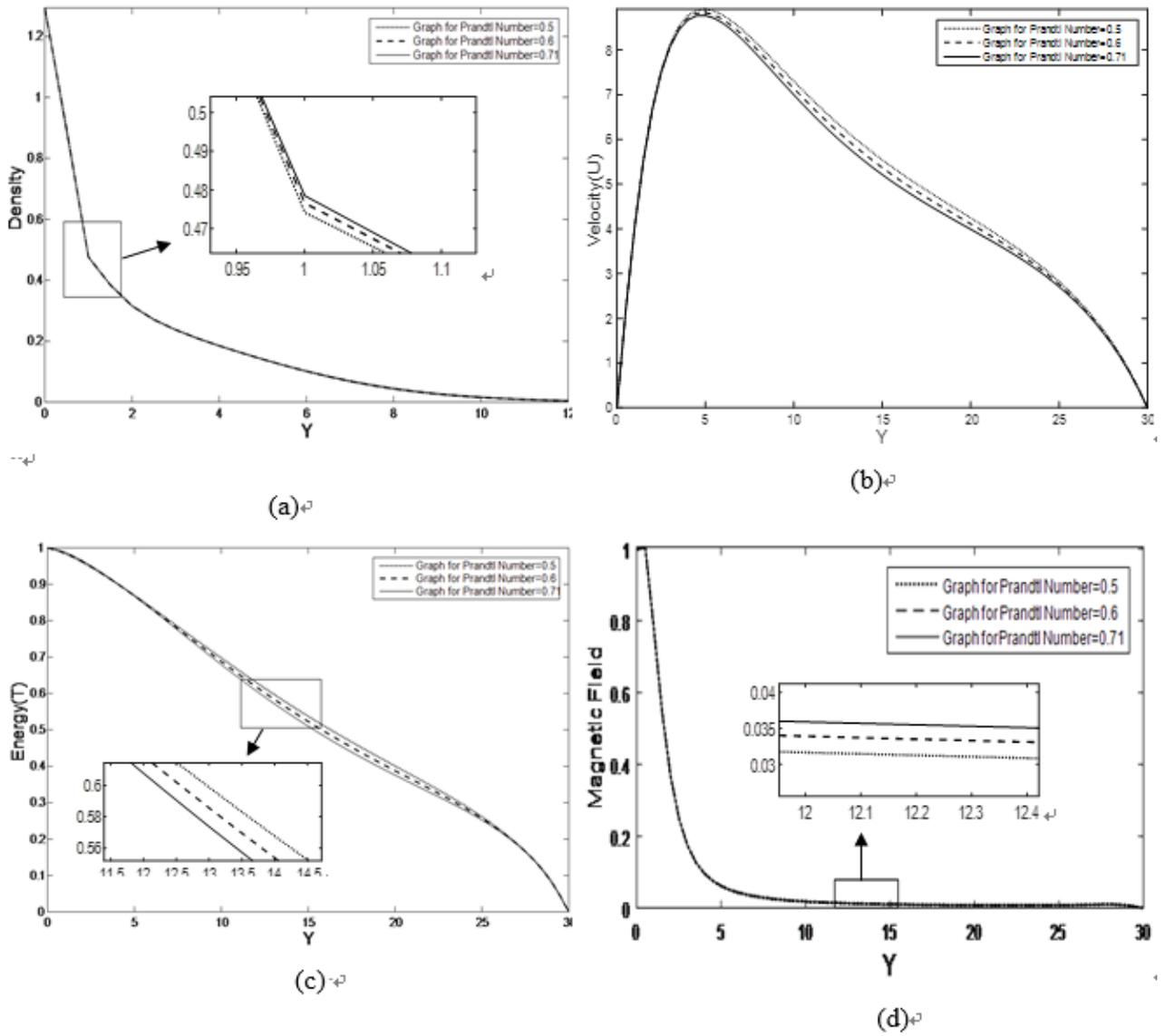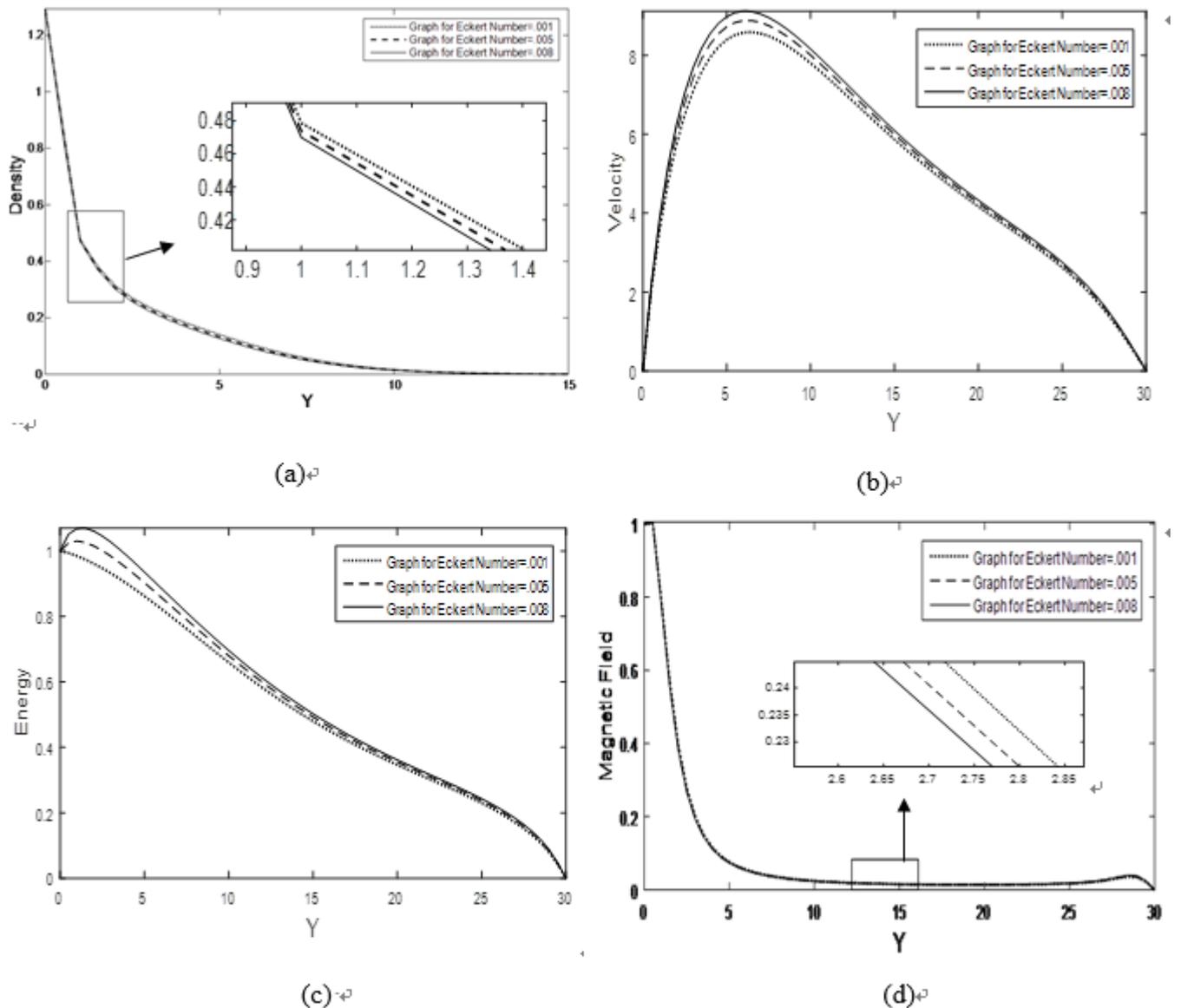
Fig. 5. Effect of Prandtl number on: (a) Density; (b) Velocity; (c) Energy; (d) Magnetic Induction,

where $M = 0.01, P_m = 1.00, k_0 = 0.21, G_r = 3.0, E_c = 0.001$, at time $\tau = 80$ (Steady state).

Figure-5 shows the profiles of velocity (U) and energy (θ) decreases with increase of Prandtl number (P_r), also the profiles of density (ρ) and magnetic induction (H) increases with increase of Prandtl number (P_r).

Fig. 6. Effect of Eckert number on: (a) Density; (b) Velocity; (c) Energy; (d) Magnetic Induction, where $M = 0.01, P_m = 1.00, k_0 = 0.21, G_r = 3.0, P_r = 0.71$, at time $\tau = 80$ (Steady state).

Figure-6 shows the density profiles (ρ) decreases with increase of Eckert number (E_c), also the profiles of velocity (U), energy (θ) and magnetic induction (H) increases with increase of Prandtl number (P_r).

Finally, qualitative and quantitative comparisons of the present steady-state results with the published results of Islam et al. (2016) are presented in Fig 7-8.
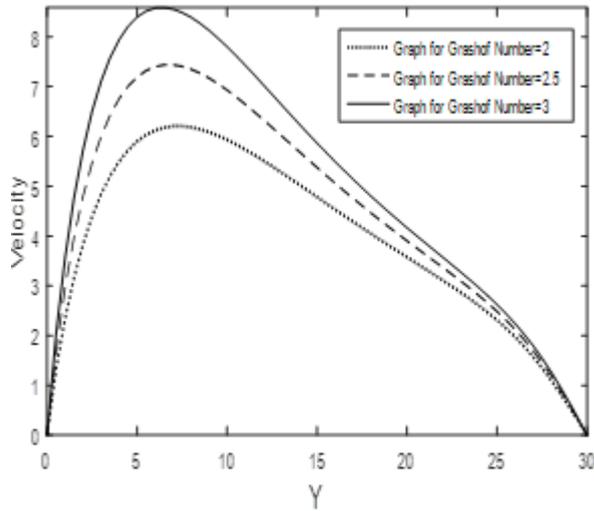
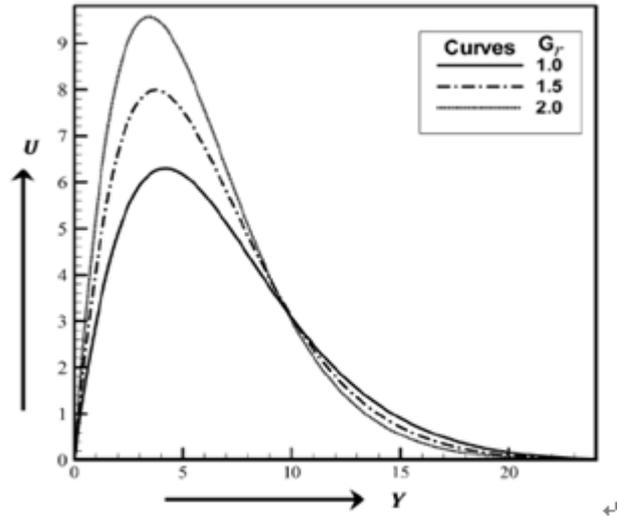Fig. 7. Velocity profiles of the present study with the presence of density.

Fig. 8. Velocity profiles of the study of Islam et al. (2016) in absence of density.

Thus the present results are qualitatively as well as quantitatively quite different with the results of Islam et al. (2016) due to compressible and incompressible fluid respectively.

For the basis of many scientific and engineering applications for investigating more complex vertical problems involving the flow of conducting fluids, it is hoped that the present investigation of the study of flow over a vertical surface can be utilized in applied physics. It is expected that the results of the present investigations be also of great interest in geophysical and astrophysical problems.

Conclusion

In this research, the explicit finite difference solution of unsteady viscous compressible fluid flow along a porous plate with induced magnetic field has been investigated for steady state solution. The results were discussed for different values of important parameters as Grashof number (G_r), Prandtl number (P_r), Eckert number (E_c) and for brevity, the effect of Magnetic diffusivity number (P_m), Magnetic force number (M) and permeability of Porous plate (k_0) are not shown. The physical properties are illustrated graphically for different values of corresponding parameters. Among them some important findings of this investigation are point out here;

1. The density decreases with increase of G_r and E_c both also increases with increase of P_r.

2. The velocity decreases with increase of P_r also increases with the increase of G_r and E_c

both.

3. The energy decreases with increase of G_r and P_r both also increases with the increase of E_c.

4. The magnetic induction decreases with increase of G_r also increases with the increase of P_r and E_c both.

References

1. M.M. Alam, M.D. Hossain, M.A. Samad, MHD free convection and mass transfer flow through a vertical oscillatory porous plate in a rotating porous medium with hall, ion-slip currents and heat source, 2016, AMSE journals –Series: Modelling B, Vol. 85, no. 1, pp. 28-42.

2. M.M. Alam, R. Pervin, Fluid flow through parallel plates in the presence of hall current with inclined magnetic field in a rotating system, 2015, AMSE journals –Series: Modelling B, Vol. 84, no. 1, pp. 49-68.

3. M.M. Alam, A. Quader, Effects of hall current and viscous dissipation on MHD free convection fluid flow in a rotating system, 2015, AMSE journals –Series: Modelling B, Vol. 83, no. 1, pp. 110-128.

4. M.M. Alam, M.M. Rahman, M.A. Samad, Dufour and soret effects on unsteady MHD Free convection and mass transfer flow past a vertical porous medium, 2006, Nonlinear Analysis: Modelling and Control, vol. 11, pp. 217-226.

5. M.M. Alam, M.A. Sattar, Transient MHD heat and mass transfer flow with thermal diffusion in a rotating system, 1999, Journal of Energy, Heat and Mass Transfer, vol. 21, no. 1, pp. 9-21.

6. M.S. Alam, M.M. Rahman, M.A. Samad, Numerical study of the combined free forced convection and mass transfer flow past a vertical porous plate in a porous medium with heat generation and thermal diffusion, 2006, Nonlinear analysis: Modeling and Control, vol. 11, No. 4, pp. 331–343.

7. Chen, Combined heat and mass transfer in MHD free convection from a vertical surface with Ohmic heating and viscous dissipation, 2004, International Journal of Engineering and Science, vol. 42, pp. 699-713.

8. A. Islam, M.M. Islam, M. Rahman, L.E. Ali, M.S. Khan, Unsteady heat transform of viscous incompressible boundary layer fluid flow through a porous plate with induced magnetic field, 2016, Journal of Applied Mathematics and Physics, vol. 4, pp. 294-306.

9. N.G. Kafoussias, MHD thermal-diffusion effects on free-convective and mass transfer flow over an infinite vertical moving plate, 1991, Astrophysics and Space Science, Springer, Vol. 192, pp. 11-19.

10. B.C. Sakiadis, Boundary layer behavior on continuous solid surfaces: Boundary layer equations for two dimensional and axisymmetric flow, 1961, American Institution of Chemical Engineering Journal, vol. 7, pp. 26-28.

11. V.M. Soundalgekar, T.V.R. Murty, Heat transfer in flow past a continuous moving plate with variable temperature, 1980, Wärme - und Stoffübertragung, Springer, vol. 14, No. 2, pp. 91–93.